Published in final edited form as:

Genesis. 2020 May ; 58(5): e23357. doi:10.1002/dvg.23357.

CRISPR/Cas9 engineering of albino cystinuria type A mice

Thomas M. Beckermann[1], **Richard C. Welch**[1], **Felisha M. Williams**[1], **Douglas P. Mortlock**[4], **Feng Sha**[1], **Talat Alp Ikizler**[1,2], **Lauren E. Woodard**[1,2,4], **Matthew H. Wilson**[*,1,2,3]

[1]Department of Medicine, Division of Nephrology and Hypertension, Vanderbilt University Medical Center, Nashville, TN 37232;

[2]Department of Veterans Affairs, Tennessee Valley Health Services, Nashville, TN, 37212;

[3]Department of Pharmacology, Vanderbilt University Nashville, TN, 37232;

[4]Department of Molecular Physiology and Biophysics, Vanderbilt University, Nashville, TN, 37232

Abstract

Cystinuria type A is a relatively common genetic kidney disease occurring in 1 in 7,000 people worldwide that results from mutation of the cystine transporter rBAT encoded by *Slc3a1*. We used CRISPR/Cas9 technology to engineer cystinuria type A mice via genome editing of the C57BL/6NHsd background. These mice are an improvement on currently available models as they are on a coisogenic genetic background and have a single defined mutation. In order to use albinism to track Cas9 activity, we co-injected gRNAs targeting *Slc3a1* and tyrosinase (*Tyr*) with Cas9 expressing plasmid DNA into mouse embryos. Two different *Slc3a1* mutational alleles were derived, with homozygous mice of both demonstrating elevated urinary cystine levels, cystine crystals, and bladder stones. We used whole genome sequencing to evaluate for potential off-target editing. No off-target indels were observed for the top ten predicted off-targets for *Slc3a1* or *Tyr*. Therefore, we used CRISPR/Cas9 to generate coisogenic albino cystinuria type A mice that could be used for *in vivo* imaging, further study, or developing new treatments of cystinuria.

Keywords

cystinuria; CRISPR/Cas9; tyrosinase; urolithiasis; albino

1 INTRODUCTION

Cystinuria occurs in 1 in 7,000 globally (Edvardsson et al., 2013). Cystinuria type A results from mutation of *SLC3A1* (rBAT protein) and type B results from mutation of *SLC7A9* ($b^{0,+}$AT protein) (Eggermann, Venghaus, & Zerres, 2012; Sahota, Tischfield, Goldfarb, Ward, & Hu, 2019). Cystinuria is autosomal recessive. High levels of cystine are found in

[*]**Correspondence to:** Matthew H. Wilson M.D., Ph.D. Associate Professor, Department of Medicine, Division of Nephrology and Hypertension, Vanderbilt University Medical Center, 1161 21st Ave South, S-3223 MCN, Nashville, TN 37232, 615-343-6348, matthew.wilson@vumc.org.

Data accessibility statement

All data and mouse strains described in this publication are available from the authors. WGS reads for WT, c.526insTT and c.527_531delTTGAG;insA mice are publicly available at GenBank (www.ncbi.nlm.nih.gov/genbank) using BioProject ID PRJNA599482.

the urine due to defective reabsorption of cystine in the proximal tubule of the kidney. Cystinuria is associated with a high number of surgical procedures, flank pain, chronic urinary tract infections, and chronic kidney disease. Available therapies for cystinuria are lacking in efficacy so animal models in which to test new therapies are needed.

Cystinuria manifests a prominent pediatric phenotype, contributing up to 10% of urolithiasis in children (Claes & Jackson, 2012; Knoll, Zollner, Wendt-Nordahl, Michel, & Alken, 2005). Onset can occur as early as between infancy and two years of age, though median onset is in the early teen years for both male and female patients (Rogers, Kalakish, Desai, & Assimos, 2007). Males are more likely to exhibit the cystinuria phenotype with symptoms before the age of three than females (Rogers et al., 2007), and males tend to do overall worse than females (Claes & Jackson, 2012).

Three different mouse models of cystinuria type A exist (Sahota et al., 2019). One was discovered after ENU mutagenesis resulting in D140G in C3HeB/FeJ mice (Peters et al., 2003), one exists as a spontaneous mutation of E383K in 129S2/SvPasCrl mice (Livrozet et al., 2014), and another was derived from homologous recombination and deletion of exon 1 in C57BL/6J-129/SvJ mice (Ercolani et al., 2010). All of these cystinuria type A strains are on mixed genetic backgrounds. Neither of the point mutation models are available to investigators in the United States. The Ercolani model which is available to U.S. investigators is not useful for testing correction by homologous recombination with Cas9 and related RNA-programmable nuclease systems.

With the goal of using cystinuria type A as a model system for eventual kidney-directed gene therapy strategies, we desired to generate a coisogenic cystinuria type A mouse strain. We created albino mice through mutation of the tyrosinase gene because they would be optimal for *in vivo* imaging of transgene expression in the whole animal, as darker coat color inhibits detection of luciferase and fluorescent proteins (Bell et al., 2007; Belur, Podetz-Pedersen, Frandsen, & Mcivor, 2007). Lastly, we desired cystinuria type A mice with mutations that could be potentially repaired via genome editing in order that we might test such strategies in an *in vivo* model. Such strategies could not be recapitulated in a mouse model created by the previously traditional model of knock-in of an antibiotic resistance cassette. For all these reasons, we undertook these studies in order to create a coisogenic albino cystinuria type A mouse line.

2 RESULTS AND DISCUSSION

We previously characterized the metabolic consequences of cystinuria type A on a mixed genetic background (Woodard et al., 2019). We sought to develop a cystinuria type A model on a coisogenic background that would be albino for *in vivo* imaging. Given speed, precision, and lower cost, we used a CRISPR/Cas9 genome editing approach to simultaneously create *Slc3a1*$^{-/-}$/*Tyr*$^{-/-}$ mice on the C57BL/6NHsd background. The strategy involved simultaneous targeting of exon 2 of *Slc3a1* (Figure 1a) and exon 1 of *Tyr*. We reasoned that *Tyr* knockout would allow us to easily identify mice wherein genome editing had occurred, allowing us to use coat color as a readout of genome editing and a surrogate marker of simultaneous *Slc3a1* editing. We first evaluated the ability of our

designed gRNA to mediate editing of *Slc3a1* in mouse embryonic fibroblast NIH3T3 cells. Surveyor assay analysis revealed editing of *Slc3a1* when the gRNA was present in the pX330-U6-Chimeric-BB-CBh-hSpCas9 (pX330-*Slc3a1*) plasmid (Figure 1b).

Pronuclear microinjection of pX330-*Slc3a1* and pX330-*Tyr* ultimately produced 14 pups of which 6 were black, 2 were mosaic, and 6 were albino. White coat color of the pups indicated gene editing activity via albinism conferred by editing *Tyr*. Analysis of black pups revealed no editing of *Slc3a1*. White pups were analyzed via TIDE analysis and two *Slc3a1* mutations were identified being c.527_531delTTGAG;insA (p.Val176GluX13) and c.526insTT (p.Glu177LeuX14) (Figure 2) (protein sequence of WT and mutations in Supporting Information). Both indels resulted in frameshift mutation in exon 2 expected to disrupt the *Scl3a1* transcript. The two different mutations were subsequently bred to homozygosity for further analysis (Figure 2b and c).

Cystinuria type A mice exhibit on average a 51-fold elevation in urinary cystine concentration (Figure 3a). We confirmed cystinuria in the c.527_531delTTGAG;insA and c.526insTT male and female mice using HPLC as described previously (Woodard et al., 2019). Both mutant *Slc3a1*−/− lines exhibited pathognomonic hexagonal cystine crystals in their urine (Figure 3b). Elevated urinary cystine and cystine crystalluria confirmed functional knockout of *Slc3a1*. Cystinuria type A mice have previously been demonstrated to form bladder stones which can be visualized by X-ray analysis (Ercolani et al., 2010; Woodard et al., 2019). Therefore, we evaluated the male and female mice of the two different mutations overtime in their ability to form bladder stones (Figure 4a and b). Both c.527_531delTTGAG;insA and c.526insTT male *Slc3a1*−/− mice exhibited a higher rate of stone formation compared to their female counterparts (Figure 4b). We did not observe stone formation in c.527_531delTTGAG;insA female mice. The c.526insTT female mice exhibited a statistically lower rate of stone formation compared to male knockout mice ($p=0.037$), though the rate was not statistically different from c.527_531delTTGAG;insA female mice or WT animals ($p=0.25$) (Figure 4b). Without doing a side-by-side comparison, the age of onset of stone formation appeared similar to that reported for other cystinuria type A strains (Zee et al., 2017).

We used whole genome sequencing to evaluate for off-target editing. We analyzed the top 10 potential off-target sites as scored by the CRISPR Finder tool (http://www.sanger.ac.uk/htg/wge/) for Cas9 cleavage activity for each gRNA (*Slc3a1* and *Tyr*) revealed no off-target editing (Supporting Information). We used Venny 2.1.0 (https://bioinfogp.cnb.csic.es/venny) to evaluate for overlap of indels between c.526insTT and c.527_531delTTGAG;insA strains (Supporting Information). Importantly, indels for *Scl3a1* and *Tyr* were present in both strains (Table). Given that the other overlapping indels did not correlate with predicted off-targets, our conclusion is that these indels are likely resultant from spontaneous mutation and subsequent breeding (Montoliu & Whitelaw, 2018).

In conclusion, we have successfully generated new cystinuria type A albino mouse models using CRISPR/Cas9 genome editing. These coisogenic strains can be used for new therapeutic approaches directed at cystinuria (Sahota et al., 2019; Zee et al., 2017), and for *in vivo* imaging of drugs or delivery vectors targeting the underlying genetic disease.

3 MATERIALS AND METHODS

3.1 Generation of *Slc3a1*$^{-/-}$/*Tyr*$^{-/-}$ mice using CRISPR/Cas9 gene editing

The pX330-U6-Chimeric-BB-CBh-hSpCas9 plasmid, which contains a human codon-optimized SpCas9 and chimeric gRNA, was used for gene editing (Addgene, #42230) (Cong et al., 2013). Exon 2 of *Slc3a1* was retrieved from the Mouse Dec. 2011 GRCm38/mm10 assembly on the UCSC genome browser (https://genome.ucsc.edu/cgi-bin/das/mm9/dna?segment=chr17:85431783,85431963). The gRNA sequence AGACTTCAGATACGCTGTTG, was subcloned into pX330 to create pX330-*Slc3a1* with the primers SLCex2g1top CACCGAGACTTCAGATACGCTGTTG and SLCex2g1bottom AAACCAACAGCGTATCTGAAGTCTC. Gene editing of mouse *Slc3a1* was confirmed by transfecting pX330-*Slc3a1* into NIH3T3 cells using Lipofectamine 2000 (Fisher, Waltham, MA) and an IDT Surveyor Mutation detection kit (Integrated DNA Technologies, Coralville, IA), similar to how we have described previously (Luo et al., 2017). The gRNA sequence targeting *Tyr*, CCATGGATGGGTGATGGGAGTCC, was subcloned into pX330 to created pX330-*Tyr*. All plasmids were confirmed using DNA sequencing. Microinjections were completed using 5 ng/μl pX330-*Slc3a1* + 5 ng/μl pX330-*Tyr*. Three pronuclear microinjection days were completed using C57BL/6NHsd mice (Envigo, Indianapolis, IN). 341 embryos were injected, 270 embryos survived (79% survival), 12 embryo transfer surgeries were completed, 16 pups born (6%), 3 pups died, and 7 of the 13 living pups were albino.

3.2 Genotyping for Slc3a1 mutations

Genomic DNA was obtained by DNeasy (Qiagen) from clipped tails from mice less than 21 days old. Primers SLC_Surv_F2 GGCTCTCCCTTCAGGTATCC and SLC_Surv_R1 TCCGTGTCCTACTCGATTGG were used for Taq PCR (Advantage 2, Clonetech) on 2 ul of each tail DNA per 20 ul PCR rxn. Thermocycling was performed with the following PCR program: Initial denature 94C for 5m, followed by 40 cycles of denature 94C for 30s, anneal 61C for 30s, and polymerize 72C for 45s, and a final polymerization of 72C for 10m to produce a 408 bp product which was gel-extracted from a 1% agarose gel. TIDE analysis (https://tide.deskgen.com/) was used to determine original genome editing events and to confirm genotypes of homozygous mice (Brinkman, Chen, Amendola, & van Steensel, 2014). Subsequently, mice were genotyped by Transnetyx (Cordova, TN).

3.3 Phenotypic analysis of mice

Urine amino acid concentrations were determined by reverse phase HPLC using a modified version of the methods of Bidlingmeyer et al. as previously described (Bidlingmeyer, Cohen, & Tarvin, 1984; Woodard et al., 2019). Urine creatinine was measured using the University of Alabama-Birmingham O'Brien Center Core C Biomarkers Laboratory by LC-MS/MS (Woodard et al., 2019). To monitor stone formation over time, mice were taken to the Vanderbilt University Institute of Imaging Science, anesthetized with isoflourane and oxygen until immobile, then placed in a Faxitron 2000 X-ray machine at setting 35 for an exposure time of 4 seconds as described previously (Woodard et al., 2019). Urinary cystine crystals were visualized using light microscopy.

3.4 Analysis of off-target Cas9 activity

Whole genome sequencing (WGS) was performed on one F3 mouse of each of the homozygous *Slc3a1*−/− alleles (c.526insTT, c.527_531delTTGAG;insA) and a WT (C57BL/6NHsd) mouse purchased from Envigo. Genomic DNA was prepared using a Dneasy kit from Qiagen (Germantown, MD) according to the manufacturers instruction. WGS and analysis was performed by Genewiz (South Plainfield, NJ). The top 10 potential off-target sites for each gRNA (*Slc3a1* and *Tyr*) were identified using the Welcome Trust Sanger Institute Genome Editing website (http://www.sanger.ac.uk/htg/wge/).

3.5 Animal care

Slc3a1$^{-/-}$ and wild type mice were bred and maintained in an AAALAC accredited vivarium at Vanderbilt University Medical Center in temperature regulated rooms (22 ± 2°C) with a 12-hour lights on-off cycle and fed as described previously (Woodard et al., 2019). All care and procedures were carried out according to the Institutional Animal Care and Use Committee of the Nashville Tennessee Valley Healthcare System VA and Vanderbilt University Medical Center. All studies were in compliance with the US National Research Council's Guide for the Care and Use of Laboratory Animals, the US Public Health Service's Policy on Humane Care and Use of Laboratory Animals, and Guide for the Care and Use of Laboratory Animals.

3.6 Statistical analysis

The T test was used for comparison urine cystine levels between groups. The log-rank Mantel-Cox test was used for survival curve (% without stones) comparison between groups.

Supplementary Material

Refer to Web version on PubMed Central for supplementary material.

ACKNOWLEDGEMENTS

This work was supported in part by Department of Veterans Affairs (BX002190 and BX004285), and National Institute of Health grant DK093660 to MHW. LEW was supported by the Department of Veterans Affairs (BX002797), the Vanderbilt O'Brien Kidney Center (5P30DK114809-02), and a career development award from the American Society for Gene and Cell Therapy. We acknowledge the Vanderbilt Transgenic Mouse/ES Cell Shared Resource (TMESCSR), now the Vanderbilt Genome Editing Resource (VGER), for assistance with pronuclear injection. The TMESCSR/VGER core is supported by the Cancer Center Support Grant (NIH CA68485), the Vanderbilt Diabetes Research and Training Center (NIH DK020593), and the Center for Stem Cell Biology.

Grant numbers: Department of Veterans Affairs (BX002190 and BX004285), and National Institute of Health grant DK093660 to MHW.

REFERENCES

Bell JB, Podetz-Pedersen KM, Aronovich EL, Belur LR, Mcivor RS, & Hackett PB (2007). Preferential delivery of the Sleeping Beauty transposon system to livers of mice by hydrodynamic injection. Nat.Protoc, 2(12), 3153–3165. [PubMed: 18079715]

Belur LR, Podetz-Pedersen K, Frandsen J, & Mcivor RS (2007). Lung-directed gene therapy in mice using the nonviral Sleeping Beauty transposon system. Nat.Protoc, 2(12), 3146–3152. [PubMed: 18079714]

Bidlingmeyer BA, Cohen SA, & Tarvin TL (1984). Rapid analysis of amino acids using pre-column derivatization. J Chromatogr, 336(1), 93–104. [PubMed: 6396315]

Brinkman EK, Chen T, Amendola M, & van Steensel B (2014). Easy quantitative assessment of genome editing by sequence trace decomposition. Nucleic Acids Research, 42(22), e168–e168. doi:10.1093/nar/gku936 [PubMed: 25300484]

Claes DJ, & Jackson E (2012). Cystinuria: mechanisms and management. Pediatr Nephrol, 27(11), 2031–2038. doi:10.1007/s00467-011-2092-6 [PubMed: 22281707]

Cong L, Ran FA, Cox D, Lin S, Barretto R, Habib N, … Zhang F (2013). Multiplex genome engineering using CRISPR/Cas systems. Science, 339(6121), 819–823. doi:10.1126/science.1231143 [PubMed: 23287718]

Edvardsson VO, Goldfarb DS, Lieske JC, Beara-Lasic L, Anglani F, Milliner DS, & Palsson R (2013). Hereditary causes of kidney stones and chronic kidney disease. Pediatric Nephrology, 28(10), 1923–1942. doi:10.1007/s00467-012-2329-z [PubMed: 23334384]

Eggermann T, Venghaus A, & Zerres K (2012). Cystinuria: an inborn cause of urolithiasis. Orphanet J Rare Dis, 7, 19. doi:10.1186/1750-1172-7-19 [PubMed: 22480232]

Ercolani M, Sahota A, Schuler C, Yang M, Evan AP, Reimer D, … Levin RM (2010). Bladder outlet obstruction in male cystinuria mice. Int.Urol.Nephrol, 42(1), 57–63. [PubMed: 19484501]

Knoll T, Zollner A, Wendt-Nordahl G, Michel MS, & Alken P (2005). Cystinuria in childhood and adolescence: recommendations for diagnosis, treatment, and follow-up. Pediatr Nephrol, 20(1), 19–24. doi:10.1007/s00467-004-1663-1 [PubMed: 15602663]

Livrozet M, Vandermeersch S, Mesnard L, Thioulouse E, Jaubert J, Boffa JJ, … Letavernier E (2014). An animal model of type A cystinuria due to spontaneous mutation in 129S2/SvPasCrl mice. Plos One, 9(7), e102700. doi:10.1371/journal.pone.0102700 [PubMed: 25048459]

Luo W, Galvan DL, Woodard LE, Dorset D, Levy S, & Wilson MH (2017). Comparative analysis of chimeric ZFP-, TALE- and Cas9-piggyBac transposases for integration into a single locus in human cells. Nucleic Acids Res, 45(14), 8411–8422. doi:10.1093/nar/gkx572 [PubMed: 28666380]

Montoliu L, & Whitelaw CBA (2018). Unexpected mutations were expected and unrelated to CRISPR-Cas9 activity. Transgenic Res, 27(4), 315–319. doi:10.1007/s11248-018-0081-2 [PubMed: 29855762]

Peters T, Thaete C, Wolf S, Popp A, Sedlmeier R, Grosse J, … Schlueter V (2003). A mouse model for cystinuria type I. Human Molecular Genetics, 12(17), 2109–2120. [PubMed: 12923163]

Rogers A, Kalakish S, Desai RA, & Assimos DG (2007). Management of cystinuria. Urol Clin North Am, 34(3), 347–362. doi:10.1016/j.ucl.2007.04.006 [PubMed: 17678985]

Sahota A, Tischfield JA, Goldfarb DS, Ward MD, & Hu L (2019). Cystinuria: genetic aspects, mouse models, and a new approach to therapy. Urolithiasis, 47(1), 57–66. doi:10.1007/s00240-018-1101-7 [PubMed: 30515543]

Woodard LE, Welch RC, Veach RA, Beckermann TM, Sha F, Weinman EJ, … Wilson MH (2019). Metabolic consequences of cystinuria. BMC Nephrol, 20(1), 227. doi:10.1186/s12882-019-1417-8 [PubMed: 31221135]

Zee T, Bose N, Zee J, Beck JN, Yang S, Parihar J, … Kapahi P (2017). alpha-Lipoic acid treatment prevents cystine urolithiasis in a mouse model of cystinuria. Nat Med, 23(3), 288–290. doi:10.1038/nm.4280 [PubMed: 28165480]

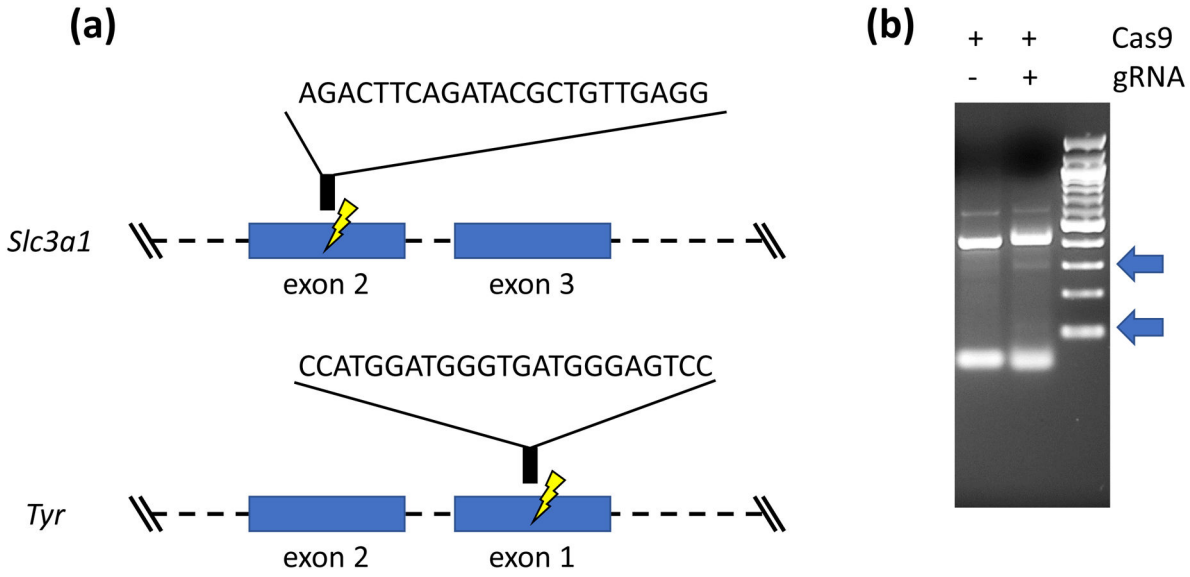

FIGURE 1.

Design and confirmation of genome editing of *Slc3a1* and *Tyr*. (a), gRNA targeting strategy of exon 2 (blue box) of *Slc3a1* and exon 1 (blue box) of *Tyr*. (b), confirmation of genome editing of *Scl3a1* via surveyor assay after attempted editing in NIH3T3 cells.

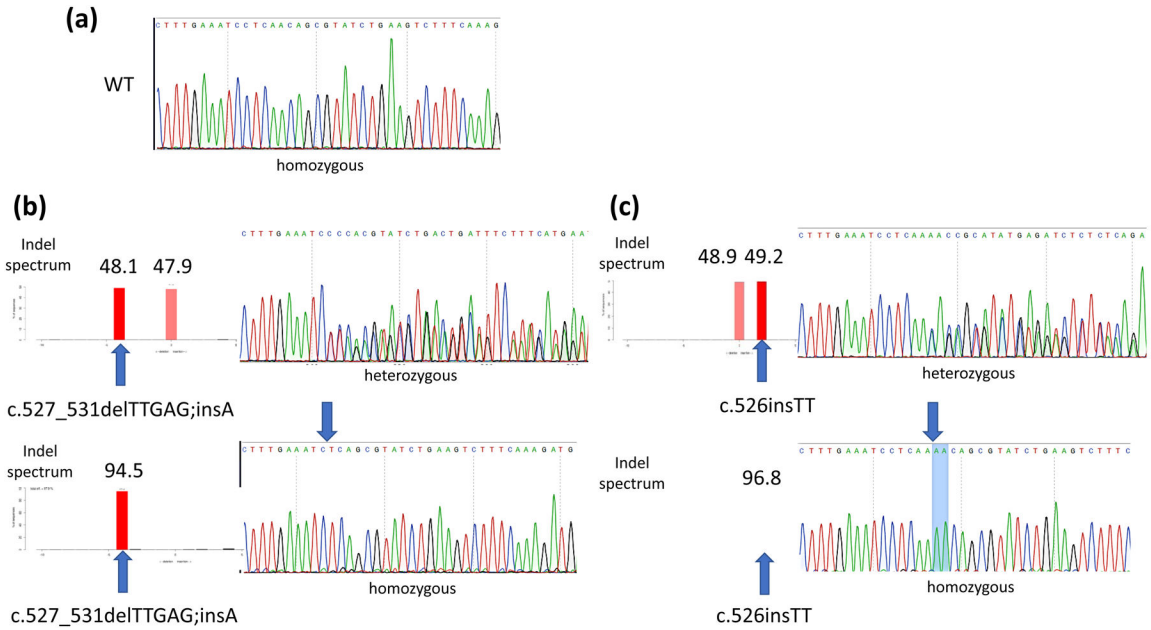

FIGURE 2.

Generation of *Slc3a1* knockout alleles. (a), TIDE analysis of WT mouse. (b) TIDE analysis of heterozygous and homozygous c.527_531delTTGAG;insA allele. (c), TIDE analysis of heterozygous and homozygous c.526insTT allele. Sequencing analysis demonstrates the complementary strand.

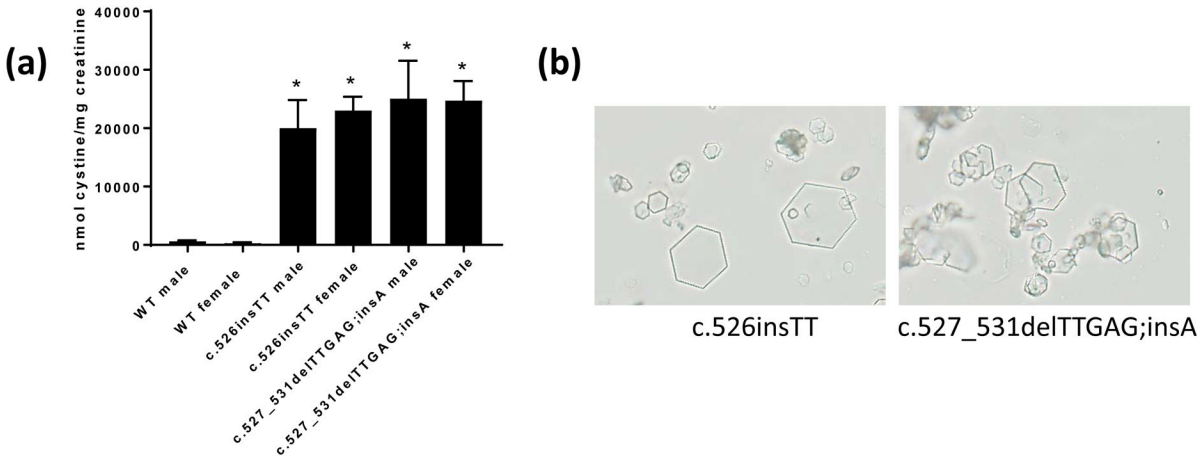

FIGURE 3.

Slc3a1 genome editing results in cystinuria. (a), urinary cystine concentration at 8–12 weeks of age in male or female WT, c.526insTT, or c.527_531delTTGAG;insA mice (N=3–10±SEM). *, $p<0.05$ via T test. (b), pathognomonic hexagonal urinary cystine crystals found in the urine of c.526insTT and c.527_531delTTGAG;insA allele animals at 8 weeks of age.

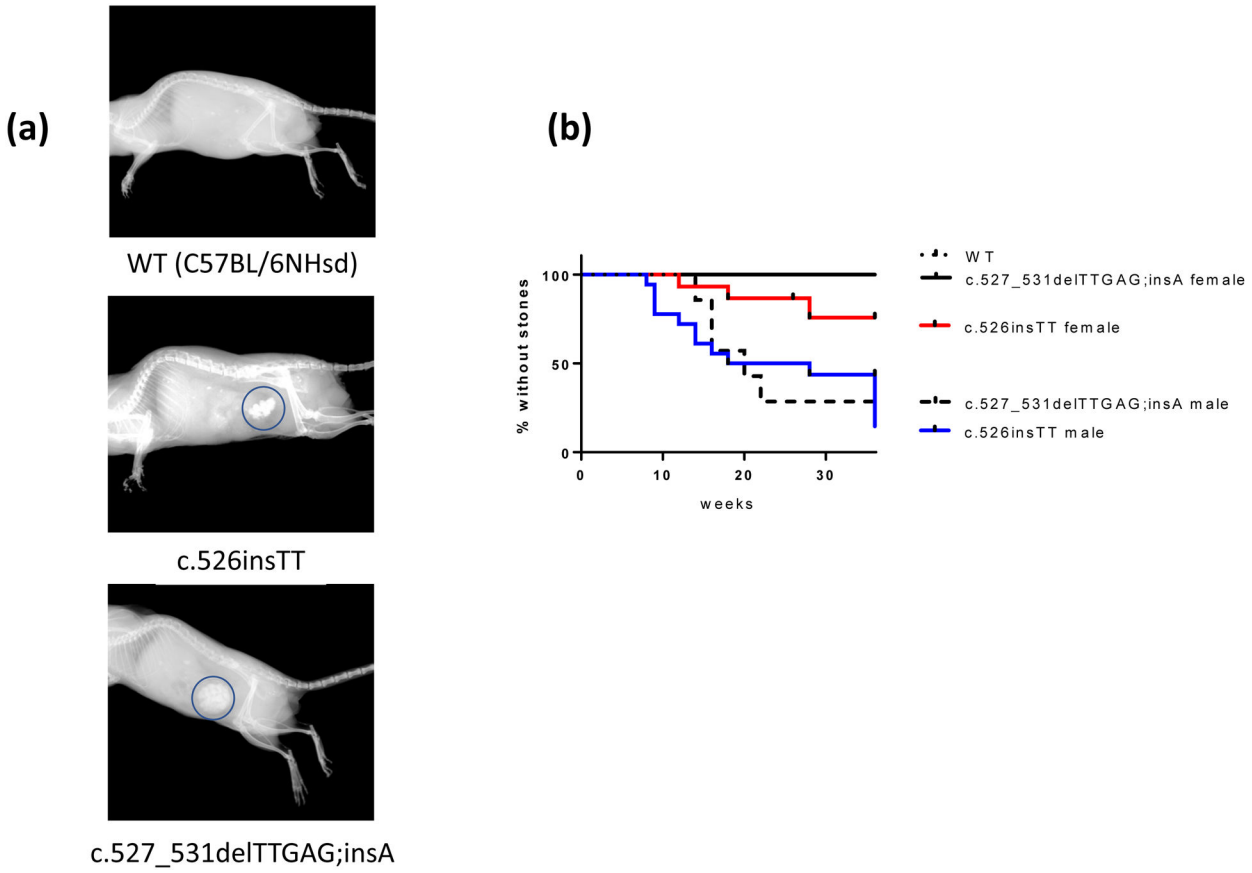

FIGURE 4.

Slc3a1 editing results in bladder stone formation. (a), X-ray analysis of a typical c.526insTT or c.527_531delTTGAG;insA male mouse. Bladder stones are outlined by the blue circles. A WT (C57BL/6NHsd) mouse is shown as a control. (b), analysis of stone formation over time (N=5–17). *Slc3a1*−/− male mice exhibited a higher rate of stone formation overtime compared to female *Slc3a1*−/− mice (log-rank Mantel-Cox test).

Table

Indels common to c.526insTT and c.527_531delTTGAG;insA strains.

Ensembl Gene	c.526insTT	c.527_531delTTGAG;insA	Gene Symbol
ENSMUSG00000044783	nonframeshift deletion	nonframeshift deletion	Hjurp
ENSMUSG00000063681	frameshift deletion	frameshift deletion	Crbl
ENSMUSG00000006412	frameshift deletion	frameshift deletion	Pfdn2
ENSMUSG00000052563	frameshift insertion	frameshift insertion	D930048N14Rik
ENSMUSG00000006056	frameshift insertion	frameshift insertion	Calcoco2
ENSMUSG00000072812	frameshift deletion	frameshift deletion	Ahnak2
ENSMUSG00000089901	frameshift deletion	frameshift deletion	Gm8113
ENSMUSG00000022255	frameshift deletion	frameshift deletion	Mtdh
ENSMUSG00000094296	frameshift deletion	frameshift deletion	Gm21798
ENSMUSG00000045350	nonframeshift deletion	nonframeshift deletion	Faml86a
ENSMUSG00000001870	frameshift deletion	frameshift deletion	Ltbpl
ENSMUSG00000024131	**frameshift insertion**	**frameshift deletion**	**Slc3al**
ENSMUSG00000045150	nonframeshift deletion	nonframeshift deletion	Olfi-1161
ENSMUSG00000028357	nonframeshift insertion	nonframeshift insertion	Kifl2
ENSMUSG00000043962	frameshift deletion	frameshift deletion	Thrap3
ENSMUSG00000062518	frameshift insertion	nonframeshift insertion	Zfp534
ENSMUSG00000035203	frameshift insertion	frameshift insertion	Epnl
ENSMUSG00000054676	frameshift deletion	frameshift deletion	1600014C10Rik
ENSMUSG00000004651	**frameshift deletion**	**frameshift deletion**	**Tyr**
ENSMUSG00000095891	frameshift insertion	frameshift insertion	GmlO717
ENSMUSG00000062649	stopgain	stopgain	Olfr44
ENSMUSG00000042254	frameshift deletion	frameshift deletion	Cilp
ENSMUSG00000032803	frameshift deletion	frameshift deletion	Cdv3
ENSMUSG00000079600	frameshift deletion	frameshift deletion	Gm17604

WGS results revealed common indels between the two cystinuria type A mouse lines generated. Importantly, *Slc3a1* and *Tyr* were mutated in both lines.